

Performance of the CLAS12 Silicon Vertex Tracker modules

M. A. Antonioli^a, S. Boiarinov^a, P. Bonneau^a, L. Elouadrhiri^a, B. Eng^a, Y. Gotra^a, E. Kurbatov^b, M. Leffel^a, S. Mandal^a, M. McMullen^a, M. Merkin^b, B. Raydo^a, W. Teachey^a, R. Tucker^c, M. Ungaro^a, A. Yegneswaran^a, V. Ziegler^a

^aThomas Jefferson National Accelerator Facility, Newport News, VA, USA

^bSkobeltsyn Institute of Nuclear Physics, Moscow State University, Moscow, Russia

^cArizona State University, Tempe, AZ

Abstract

For the 12 GeV upgrade, the CLAS12 experiment has designed a Silicon Vertex Tracker (SVT) using single sided microstrip sensors fabricated by Hamamatsu. The sensors have graded angle design to minimize dead areas and a readout pitch of $156\ \mu\text{m}$, with intermediate strip. Double sided SVT module hosts three daisy-chained sensors on each side with full strip length of 33 cm. There are 512 channels per module read out by four Fermilab Silicon Strip Readout (FSSR2) chips featuring data driven architecture, mounted on a rigid-flex hybrid. Modules are assembled on the barrel using unique cantilevered geometry to minimize amount of material in the tracking volume. Design and performance of the SVT modules are presented, focusing on results of electrical measurements.

Keywords: Tracking and position-sensitive detectors, Solid-state detectors, Hybrid integrated circuits

1. Introduction

The Continuous Electron Beam Accelerator Facility's (CEBAF) Large Acceptance Spectrometer (CLAS) is being upgraded for the 12 GeV electron beam to conduct spectroscopic studies of excited baryons and of polarized and unpolarized quark distributions, investigations of the influence of nuclear matter on propagating quarks, and measurements of Generalized Parton Distributions (GPDs). Deep exclusive reactions, in which an electron scattering results in a meson-baryon final state, provide stringent requirements for the CLAS12 tracking system (see Fig. 1). The central tracker consists of a solenoid, Central Time-Of-Flight system (CTOF), and Silicon Vertex Tracker (SVT). The SVT will be centered inside of the solenoid, which has 5 T magnetic field.

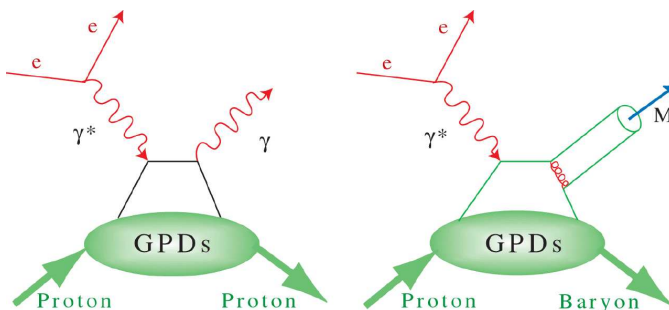


Figure 1: The handbag diagram for deeply virtual Compton scattering (left), and for deeply virtual meson production (right). Four GPDs describe the soft proton structure part. They depend not only on longitudinal momentum fraction x , but on two more variables: the momentum imbalance of the quark before and after the interaction, and the momentum transfer to the proton.

2. SVT Physics requirements

Essential parts of the physics program, such as GPDs, require tracking of low momentum particles with few percent momentum and about one degree angle resolution at large angles [1]. This is achieved by the SVT. Silicon detector technology makes an excellent match to the central tracking system in the CLAS12 configuration, small space and high luminosity operation that is needed for accurate measurements of exclusive processes at high momentum transfer. SVT provides standalone tracking capabilities in the central detector region:

- Measure recoil baryons and large angle pions, kaons
- Polar angle (θ) coverage: 35° – 125°
- Azimuthal angle (ϕ) coverage: $\geq 90\%$ of 2π
- Momentum resolution: $\delta p_T/p_T \leq 5\%$
- Angle resolution: $\delta\theta \leq 10$ – 20 mrad, $\delta\phi \leq 5$ mrad
- Tracking efficiency: $\geq 90\%$
- Match up tracks with hits in the CTOF for β vs. p measurement (particle ID)
- Reconstructing detached vertices, e.g. $K_s \rightarrow \pi^+\pi^-$, $\Lambda \rightarrow \pi^-p$, $\Xi \rightarrow \Lambda\pi$ for efficient experimental program in strangeness physics
- Stable operation in 5 Tesla magnetic field at instantaneous luminosities $L=10^{35}\text{ cm}^{-2}\text{ s}^{-1}$

Expected integrated luminosity per year 500 fb^{-1} . Radiation dose for forward sensors (carbon target) is 2.5 Mrads.

3. Detector design and simulation

The current design of the Barrel Silicon Tracker (BST) comprises 33792 channels of silicon strip sensors in eight layers

43 (four concentric polygonal regions that have 10, 14, 18, and 24
 44 double sided modules mounted back to back). There are three
 45 daisy-chained sensors per layer (six per module). Each layer
 46 has 256 strips with linearly varying angles of 0° – 3° . The read-
 47 out strips have a constant ϕ pitch of $1/85^\circ$ (see Fig. 2).

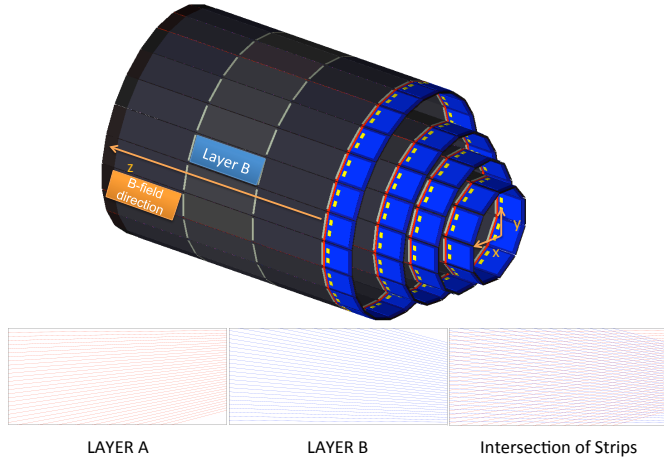


Figure 2: Side view of the SVT detector.

48 According to the results of JEANT simulation of the SVT, a
 49 resolution of $50 \mu\text{m}$ in the bending plane is needed to measure,
 50 with a precision better than 5%, tracks with momentum up to
 51 1 GeV (see Fig. 3) [2, 3, 4]. Silicon Vertex Tracker uses single
 52 sided $320 \mu\text{m}$ thick microstrip sensors fabricated by Hamamatsu.
 53 The sensors have graded angle design to minimize dead
 54 zones and a readout pitch of $156 \mu\text{m}$, with intermediate strip.

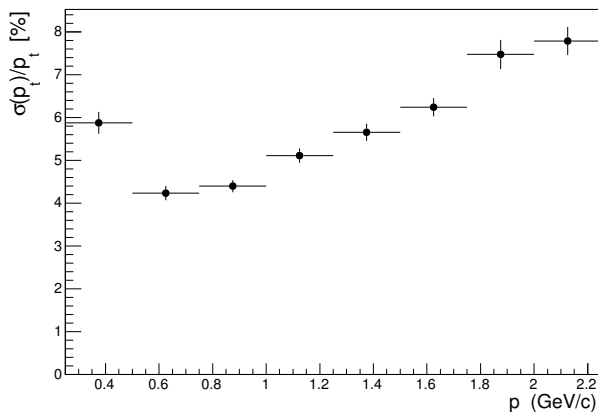


Figure 3: Results of Monte Carlo Simulation for the SVT momentum resolution.

55 4. SVT Module

56 To minimize multiple scattering a unique module design with
 57 extra long 33 cm strips has been developed to reduce material
 58 budget to 1% of radiation length per region (two silicon planes)

for normal incidence tracks, which is essential for low momen-
 60 tum tracking. The SVT modules are cantilevered off a water-
 61 chilled cold plate, designed to remove the heat generated by the
 62 electronics, located only at one end of the module (see Fig. 4).
 63 Readout electronics is outside of the tracking volume.

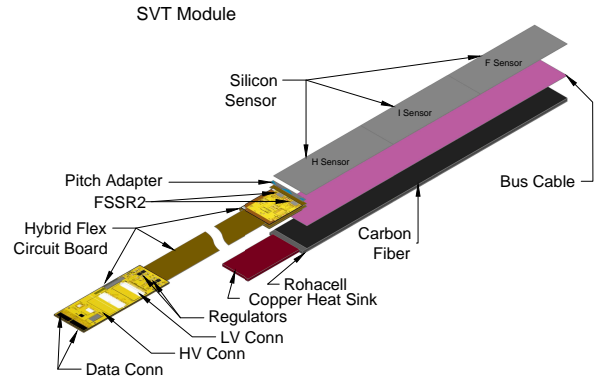


Figure 4: Layout of the SVT module.

64 Double sided SVT module hosts three single sided daisy-
 65 chained microstrip sensors fabricated by Hamamatsu on each
 66 side. All modules have 3 types of sensors: Hybrid, Intermedi-
 67 ate, and Far. Sensors are cut from 6 inch wafers, 2 sensors per
 68 wafer. All sensors have the same size, $112 \times 42 \text{ mm}$. All SVT
 69 modules are identical.

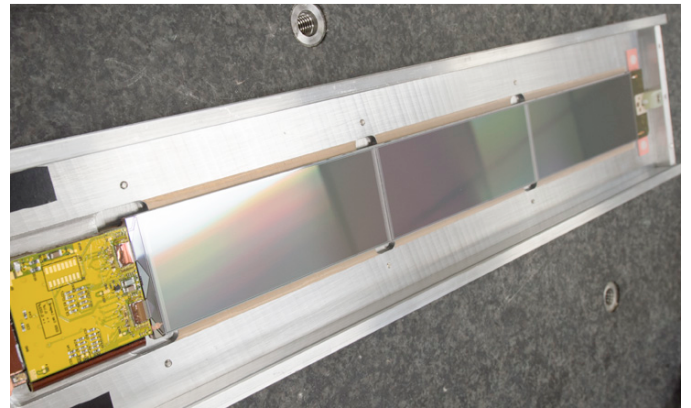


Figure 5: SVT module in the carrier box.

70 Sensors are mounted on a composite backing structure com-
 71 posed of Rohacell 71 core, bus cable, and carbon fiber. The
 72 carbon fiber skin is made from K13C2U fibers oriented in a
 73 quasi-isotropic (45/-45/0) pattern. It is co-cured with the bus
 74 cable, which is made from a Kapton sheet with 0.003-mm thick
 75 copper traces, which are 0.5 mm wide; traces on one side pro-
 76 vide high voltage to the sensors, on the other side they form a
 77 $6 \times 6 \text{ mm}$ copper mesh over the entire area for grounding the car-
 78 bon fiber. The Rohacell core under the hybrid board is replaced
 by a copper heat sink to remove $\sim 2 \text{ W}$ of heat generated by the
 ASICs. At the downstream end of the module, the Rohacell
 core is replaced by a polyether ether ketone (PEEK) core [5].

82 Pitch adapter serves to match the $156\ \mu\text{m}$ sensor readout pitch¹²⁴
 83 to the $50\ \mu\text{m}$ FSSR2 bonding pad pitch. The pitch adapter is¹²⁵
 84 a glass plate with metal traces made of an alloy of aluminum¹²⁶
 85 and copper. The alloy improves electromigration hardness and¹²⁷
 86 bonding. The metal layer is sputter deposited. The passivation¹²⁸
 87 layer protects the aluminum traces from damage and is made¹²⁹
 88 from SiO_2 [6]. There are 512 channels per module read out by¹³⁰
 89 FSSR2 chips, mounted on a hybrid (see Fig. 5).¹³¹

90 A readout system which instruments both sides of a module¹³²
 91 with a single rigid-flex Hybrid Flex Circuit Board (HFCB), has¹³³
 92 been developed by JLAB (see Fig. 6) and fabricated by Com¹³⁴
 93 punetics Inc. The HFCB is located on the upstream end of the¹³⁵
 94 module. It hosts four FSSR2 ASICs, two on the top and two on¹³⁶
 95 the bottom side. The hybrid areas are connected by a 10 mm¹³⁷
 96 long wing cable. Data is transferred from the hybrid via the flex¹³⁸
 97 cable to the level one connect (L1C) board. The L1C has two¹³⁹
 98 high density Nanonics connectors for data and control lines,¹⁴⁰
 99 Molex Micro-Fit 9-pin connector for high voltage ($\sim 85\ \text{V}$) bias¹⁴¹
 100 to the sensors, and AMP Mini CT 17 pin connector for low volt-¹⁴²
 101 age ($2.5\ \text{V}$) power to the ASICs. There are 12 layers in rigid part
 102 and 6 layers in flex part. Control, data, and clock signals do not¹⁴³
 103 cross the ground plane splits. Clock signals are located on a
 104 separate layer. Guard traces are routed between output, clock,¹⁴⁴
 105 and power lines. Separate planes are provided for analog and¹⁴⁵
 106 digital power. To reduce noise on these planes, regulators and¹⁴⁶
 107 bypass capacitors are added. High voltage filter circuits and the¹⁴⁷
 108 bridging of high and low voltage return lines are located close¹⁴⁸
 109 to the ASICs. Decoupling capacitors for power transmission¹⁴⁹
 110 are placed at transitions between flex and rigid materials.

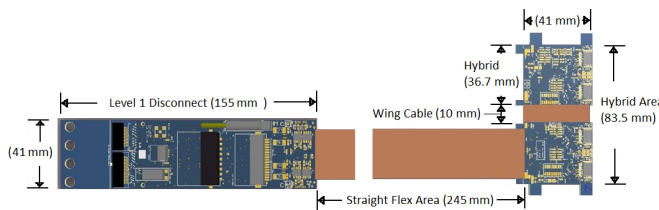


Figure 6: Hybrid Flex Circuit Board (HFCB).

111 5. Readout system

112 The FSSR2 ASIC has been developed at Fermilab for the¹⁶⁷
 113 BTeV experiment [7]. It was fabricated by Taiwan Semicon-¹⁶⁸
 114 ductor Manufacturing Company in the $0.25\text{-}\mu\text{m}$ CMOS process.¹⁶⁹
 115 The chip features a data-driven architecture (self-triggered,¹⁷⁰
 116 time-stamped). Each of the 128 input channels of the FSSR2¹⁷¹
 117 ASIC has a preamplifier, a shaper that can adjust the shaping¹⁷²
 118 time ($50\text{--}125\ \text{ns}$), a baseline restorer (BLR), and a 3-bit ADC.¹⁷³
 119 The period of the clock called beam crossing oscillator (BCO)¹⁷⁴
 120 sets the data acquisition time. If a hit is detected in one of¹⁷⁵
 121 the channels, the core logic transmits pulse amplitude, chan-¹⁷⁶
 122 nel number, and time stamp information to the data output in-¹⁷⁷
 123 terface. The data output interface accepts data transmitted by¹⁷⁸

the core, serializes it, and transmits it to the data acquisition
 system. To send the 24-bit readout words one, two, four, or six
 Low Voltage Differential Signal (LVDS) serial data lines can be
 used. Both edges of the 70 MHz readout clock are used to clock
 data, resulting in a maximum output data rate of 840 Mb/s. The
 readout clock is independent of the acquisition clock. Power
 consumption is $\leq 4\ \text{mW}$ per channel. The FSSR2 is radiation
 hard up to 5 Mrad.

Each of the four FSSR2 ASICs reads out 128 channels of
 analog signals, digitizes and transmits them to a VXS-Segment-
 Collector-Module (VSCM) card developed at Jefferson Lab.
 The event builder of the VSCM uses the BCO clock timestamp
 from the data word of each FSSR2 ASIC and matches it to the
 timestamp of the global system clock, given by the CLAS trig-
 ger. The event builder buffers data received from all FSSR2
 ASICs for a programmable latency time up to $\sim 16\ \mu\text{s}$. The
 VSCM is set up to extract event data within a programmable
 lookback window of $\sim 16\ \mu\text{s}$ relative to the received trigger.
 The trigger latency is expected to be $\sim 8\ \mu\text{s}$.

6. Calibration of the readout chain

Since the SVT modules are designed with a binary readout
 system, the analog channel response cannot be measured direct-
 ly. Instead, the analog response is reconstructed by inject-
 ing a calibration charge on the channel and measuring the cor-
 responding occupancy over a range of threshold values. Noise
 is measured using external, low frequency calibration charge
 injected in the absence of signal. The injected charge is shaped
 and amplified in the analog circuitry to form an output signal.
 The discriminator threshold determines whether or not the out-
 put signal corresponded to a hit. The probability that the in-
 jected charge produces a hit depends on the setting of the dis-
 criminator threshold. The average hit probability is measured
 by repeating the process of injecting charges and counting the
 fraction of readout triggers that produced a hit. This measure-
 ment is repeated over a range of threshold settings to produce
 an occupancy plot. The occupancy plots were measured setting
 the pulser amplitude at fixed values and changing the compar-
 ator thresholds. Each point of an occupancy plot represents the
 percentage of times that the comparator fires for a certain value
 of injected charge. In between the high and low threshold re-
 gions, the occupancy curve is described by an error function,
 or S-curve, which can be fitted to the occupancy histogram for
 each channel, producing a mean value (discriminator thresh-
 old) and standard deviation (noise). The conversion from mV
 to electrons is performed considering a nominal value for the
 FSSR2 injection capacitance of 40 fF.

Threshold dispersion is defined to be a standard deviation
 of the distribution of means obtained from the parameters of
 the complementary error function fit. The noise and threshold
 dispersion constants for each individual detector channel are
 measured and the values are used by the zero-suppression al-
 gorithms implemented in the core logic of the FSSR2 and by
 calibration procedures to identify defective channels. A com-
 parison of the noise for 33 cm strips with the threshold spread
 demonstrates that the threshold spread is negligible compared

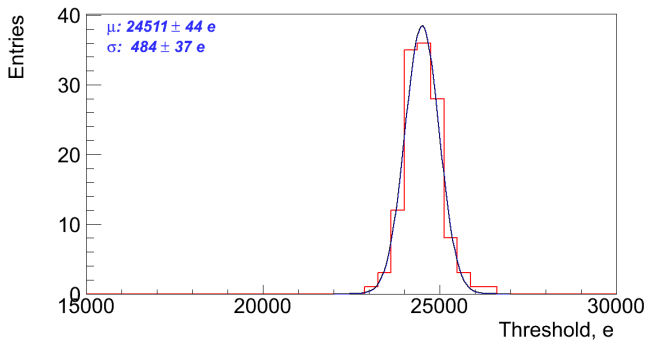


Figure 7: Typical threshold dispersion within a chip.

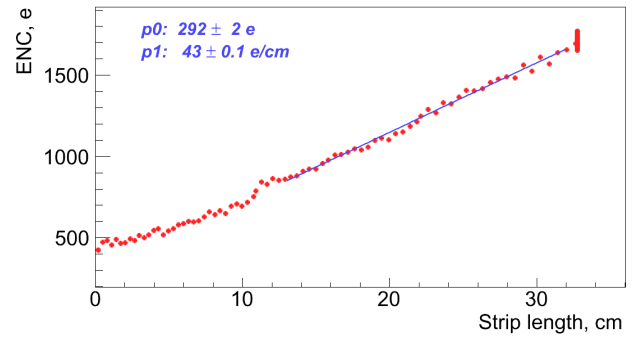


Figure 9: Input noise vs. strip length.

179 to noise and will not affect efficiency and noise occupancy (see
180 Fig. 7).

181 7. Results of the Full Chain Test

182 No significant correlated noise has been observed between
183 the channels of the same chip, between the chips of the same
184 module or between the closely placed modules. Measured av-
185 erage channel noise (see Fig. 8) is comparable with estimated
186 contributions of different noise sources.

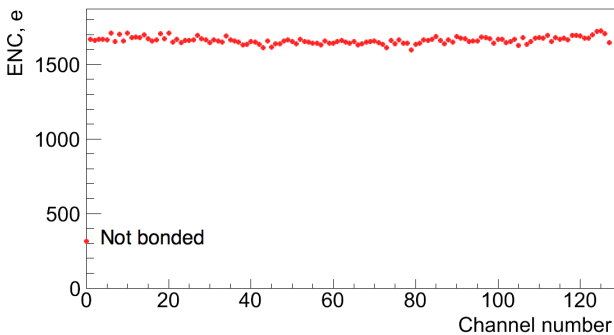


Figure 8: Typical input noise on a single chip of an SVT module.

187 Longer silicon strips have higher capacitance and thus a
188 higher expected value for the input noise (see Fig. 9). Noise cal-
189 ibration accounts for the different strip lengths and pitch adapter
190 layouts that affect the input capacitance of the preamplifier.

191 Noise occupancy histogram with no charge injection is
192 shown in Fig. 10. It probes the tail of the noise distribution,
193 which can show effects masked by the higher occupancy at
194 low thresholds. Channel noise allows setting a 3σ threshold
195 at 20 keV level.

196 SVT module performance meets physics requirements and
197 production at Fermilab is expected to start in summer of 2013
198 followed by barrel integration and commissioning in 2014.
199 SVT detector will be installed in Hall B in 2015.

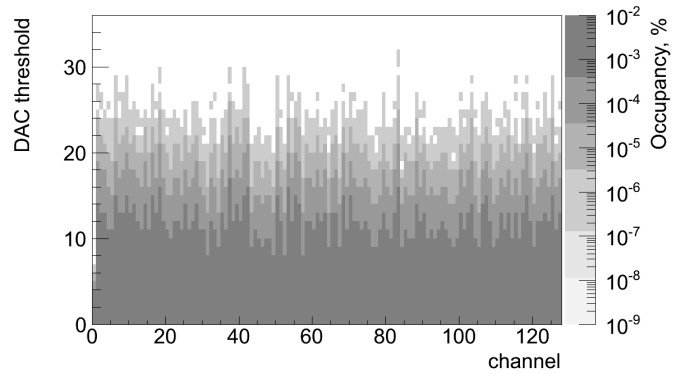


Figure 10: Channel noise occupancy vs. DAC hit/no-hit threshold (in DAC bins, one DAC bin corresponds to 3.5 mV).

200 8. Acknowledgements

201 We appreciate the contribution of J. Andresen, C. Britton, S.
202 Chappa, A. Dyer, J. Hoff, V. Re, and T. Zimmerman to the de-
203 sign of the HFCB. We are grateful to administrative, engineer-
204 ing, and technical staff of Fermilab Silicon Detector Facility for
205 excellent work on module assembly.

206 References

- 207 [1] CLAS12 Technical Design Report, 2008.
208 [2] A. Vlassov et al. CLAS-Note 2006-020. Background Study for the Cen-
209 tral Detector Planned for the 12 GeV Upgrade of CLAS.
210 [3] K. Stopani. CLAS-Note 2008-001. Momentum Resolution and Tracking
211 Efficiency Studies for the Barrel Silicon Tracker.
212 [4] CLAS12 Software - 12 GeV Upgrade, 2013.
213 [5] CLAS12 Silicon Vertex Tracker Technical Design Report, 2012.
214 [6] M. Ullan, et al. High Pitch Metal-On-Glass Technology For Pad Pitch
215 Adaptation Between Detectors And Readout Electronics, IEEE Trans. on
216 Nuclear Science, v. 51, n. 3, pp. 968-974, June 2004.
217 [7] R. Yarema, J. Hoff, A. Mekkaoui, M. Manghisoni, V. Re, P.F. Manfredi,
218 L. Ratti and V. Speziali, Fermilab silicon strip readout chip for BTEV,
219 IEEE Trans. Nucl. Sci. 52(3), 799 (2005).